Fuel cell powered octocopter for inspection of mobile cranes: Design, cost analysis and environmental impacts

Published version:

DOI:10.1016/j.apenergy.2018.02.072

(Article begins on next page)

Fuel cell powered octocopter for inspection of mobile cranes: design, cost analysis and environmental impacts

N. Belmonte[1], S. Staulo[2], S. Fiorot[3], C. Luetto[4], P. Rizzi[1*], M. Baricco[1]

[1] Department of Chemistry and NIS, University of Turin, Via Pietro Giuria 7, 10125 Turin, Italy

[2] Stones S.a.s., Via Risorgimento 1, 10093 Collegno (TO), Italy

[3] Environment park S.p.A, Via Livorno 60, 10144 Turin, Italy

[4]Tecnodelta S.r.l., Via Francesco Parigi 5/h, 10034 Chivasso (TO), Italy

* Corresponding author: paola.rizzi@unito.it

Abstract

In this paper, the possible development of a drone for mobile crane inspection is investigated. Since the flying time of the drones currently in commerce is too short for the designed application, proton exchange membrane fuel cells and lithium-ion batteries are considered as alternative power systems to extend the flying time. Both systems are analyzed from an economical point of view and a life cycle assessment is performed to identify the main contributors to the environmental impact. From a commercial point of view, the lightweight fuel cell, being a niche product, results more expensive with respect to the Li-ion battery. On the other hand, the life cycle assessment results show a lower burdens of both technologies with respect to other components of the two systems, as carbon fiber. The source of the hydrogen and the electricity mix play a critical role as well.

Keywords

Fuel Cell, Battery, Unmanned Aerial Vehicle, Life Cycle Assessment

1 Introduction

Unmanned Air Vehicles (UAVs) have traditionally been used in military operations for a number of years [1]. Recently, UAVs have generated increasing interests due to their potential application in civilian domains [2], such us glaciology [3], agriculture [4,5], monitoring of erosion phenomena [6], geothermal environments [7], surveillance of open cut mining sites [8] and archaeological areas [9]. In recent years, electric propulsion systems become popular among small or mini UAVs for several reasons, i.e. quiet operation, easy and safe handling and storage, precise power management and control [10]. The main drawback of this solution, however, is the limited flying range of the device. A lot of efforts have been dedicated to the estimation and optimization of the flying range in electrical UAVs [11,12]. As pointed out by Simic et al. [13], increasing the battery size is not a viable solution, since the weight becomes a limiting factor. Rajendran et al. [14] suggested a solar-powered UAV for areas having considerably high irradiation. In this case the device could fly ideally all the day, powered directly with the electrical current produced by the photovoltaic panels and the excess of energy can be used to charge a buffer battery. Chang et al. [15] obtained an increase of the flying range up to 17.6 % dividing the battery in small modules and introducing the possibility of dumping some exhausted modules during the flight, reducing the weight of the drone. This solution, however, is not generally applicable. In a study by Simic et al. [13] the possibility of charging the UAV on the job using wireless energy transfer (WET) is suggested. In this case, in fact, the drone might be used for inspection of power transmission lines and towers. This possibility was not tested yet on a power line, but the authors performed several lab experiments on wireless energy transfer, obtaining encouraging results. Also this solution, which still needs some further developments, is not widely applicable.

Another option to increase the flying range of a UAV is the use of a fuel cell to generate electricity. In this case, once the power is defined according to the needed features of the UAV, the only limit of the flying range is given by the amount of fuel that the device can carry. This possibility has been explored in many works: Renau et al. [16] studied the integration of a HT-PEM (high temperature PEM fuel cell) on a UAV for high altitude (about 10 km) missions, Brandley et al. [17] integrated a conventional PEM fuel cell on an unmanned aircraft for lower altitude missions, with respect to the previous case. PEM fuel cell stacks seem to be the most appropriate solution for UAVs, due to accomplished high operational parameters, reliability and commercial availability [18-20]. Dudek et al. [10] tested a hybrid PEM fuel cell and Li-ion battery system. In a study by Kim et al. [2], a PEM fuel cell is coupled to a metal hydride storage tank for application on UAVs.

A comparison of performances of battery and fuel cell systems has been reported, for both mobile [21] and stationary [22] applications. Battery systems are usually more efficient than those based on fuel cells, but require higher recharging times. Fuel cells are usually less flexible in operations, as evidenced by the need of suitable start-up procedures before reaching the best performances. Fuel cells have intrinsically higher running times, only limited by the fuel feeding. Up to date, no direct comparison between battery and fuel cell systems for UAV applications are available.

In this paper, a feasibility study is carried out to evaluate the application of a PEM fuel cell to increase the flying range for a UAV. Unlike the previous reports, however, the PEM system is considered to be set up into an octocopter instead of a monoplane. In this study, not only the planning of the system is considered, but also a cost analysis has been performed. In addition, a Life Cycle Assessment (LCA) analysis is carried out to evaluate the most important contributors to the environmental impact relative to the production of the drone and to its use. Together with the fuel cell-powered UAV, a similar battery powered device is considered, representing in fact the most used and commercially widespread technology. A comparison between the two systems is made, considering technical aspects, costs and environmental impacts.

2 Designed application

The application of the drone considered in this study is the periodical inspection of lifting equipment and cranes. These inspections have to be performed, in Italy, according to ISO 4301-2:2009 and UNI EN 13000 Mobile cranes Normative that individuate some critical components, which have to be periodically inspected by qualified technicians. To this purpose, these components are currently disassembled and put on the ground, but this procedure is expensive and time consuming. In order to avoid this step, video inspection performed by drones can be a valid alternative. This can be done by implementing a First-Person-View (FPV) system on the drone. FPV refers to the management of a remote control aircraft or vehicle while using an onboard camera that sends real-time video to either a video monitor or video goggles.

According to the application, the main features required for the drone are a high stability, a flying time of at least 120 minutes and a suitable image acquisition system. These needs address the choice towards a mini hexa or octocopter, for their higher stability with respect to quadcopters. Hexa and octocopters are more powerful with respect to quadcopters, but also heavier. These considerations, together with the need of a long flying time, require a powerful battery or, in the case of the fuel cell, not less than 1 kW power output. In both cases, the weight of the battery/fuel cell with these requirements is around 1 kg. As image acquisition system concerned, a high resolution video camera is needed, with support and transmitter onboard, with a video receiver and a screen on the ground. One of the main critical aspects of the camera is its weight, which ranges from 0.3 kg of a GoPro-type camera up to 1.5 kg for a full frame reflex camera. Further evaluations on the type of drone, as well as the power supply, will be discussed in paragraph 4.

It must be pointed out that the main purpose of this study, rather than the construction of the drone, is the evaluation of the environmental burdens associated with the manufacturing and use of a hydrogen-powered PEM fuel cell drone compared with those associated to a similar battery-powered one. Lithium-ion batteries in fact are currently the most used for propulsion of mini UAVs.

3 Tests

In order to verify the feasibility of the integration of a PEM fuel cell on a UAV to increase the flight time, a preliminary study has been carried out on the electricity consumption of UAV’s engines in different flight conditions. This allowed identifying the load variations the fuel cell undergoes. Once load variations have been identified, a bench test has been performed on the fuel cell to verify its response to the different flight conditions.

3.1 Flight tests

The flight tests were carried out with a battery-powered hexacopter, having the specifications reported in tab. 1.

UAV type	hexacopter
Nominal power per engine	380 W
Maximum power reached during the tests	360 W
Battery weight	1050 g
Empty weight	2440 g
Extra load used for the tests	1000 g

Tab. 1 Specifications of the UAV used for the tests.

It is worth noting that the main purpose of the flight tests was to identify the energy requirements of the engines in different flight conditions, and not to size the system.

The variation of the electrical current absorbed by the engines is reported in Fig. 1 as a function of the time for a flight in “dynamic” conditions (green curve) and in “normal” mode (blue line). The “dynamic” flight mode consists of sudden accelerations and quick direction changes, successions of landings and take offs, which correspond to the peaks in current intensity. It can be noticed that the absorbed electrical current is close to 20 A, but it may vary significantly in few milliseconds. The “normal” flight mode, on the other hand, consisted of a flight at constant speed after takeoff. In this case, the absorbed electrical current is almost constant at 20 A during the whole flight, except for the small changes of 5-10 A that can be associated to repositioning of the UAV.

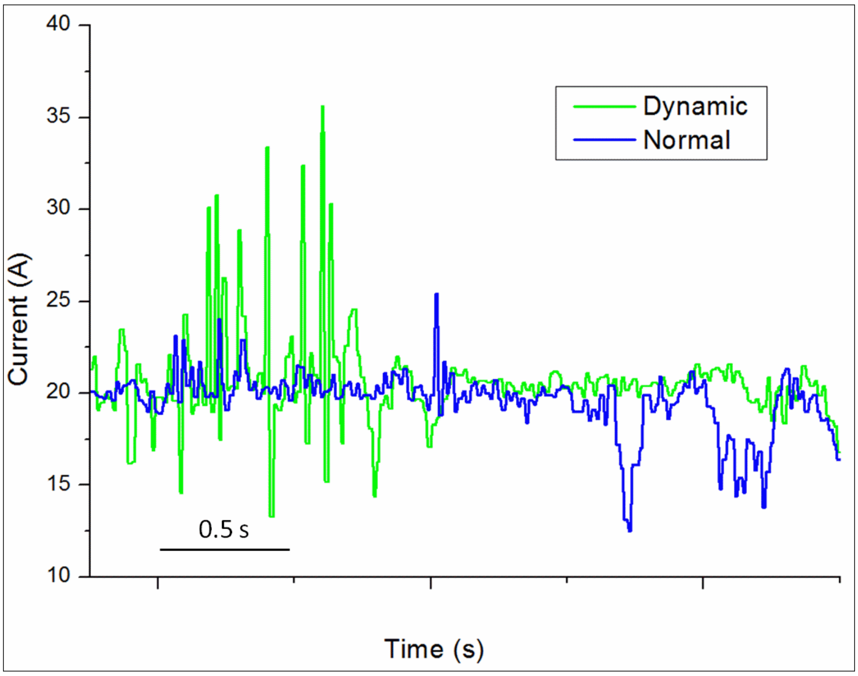

Fig. 1 Electrical current absorbed by the drone in flight “dynamic” and “normal” conditions.

The “normal” flight mode is similar to the operating conditions of the drone for the chosen application: image acquisition of structural parts of high cranes in fact implies reaching a position, which is not necessarily to be performed at the maximum speed, and keeping it for several minutes for image acquisition.

3.2 Fuel cell bench tests

Once performed the flight tests to register the load curves, a bench test was performed on a PEM fuel cell in order to verify not only the possibility of using the latter for drone power supply, but also to evaluate if electric transient dynamics are compatible with the requirements of the engines. The system is composed by a microprocessor-based controller managing contemporarily load flows between the fuel cell, the battery and the engines. There is a further part dedicated to power supply for the auxiliary components (powered by the battery).

A small battery pack is needed for the system since, as it will be shown in paragraph 3.2.3, the fuel cell is not able to follow instantly the sudden load changes dictated by the engines in certain conditions, such as sudden accelerations and direction changes of the UAV. When these conditions occur, the current required by the engines is provided by both batteries and fuel cell, also contemporarily, as will be described in paragraph 3.2.2. This is done by a DC/DC converter, which has 3 separated inputs: fuel cell, engines and battery. On the fuel cell side, an algorithm verifies the correct running of the fuel cell, comparing the instant state with the polarization curve set by the user, and makes the produced current available taking it with 10 A/s transients in order not to damage the fuel cell. For the same reason, when the power demand by the engines decreases, the current produced by the fuel cell is not suddenly reduced, but used for battery pack charging.

3.2.1 Test apparatus

The following devices composed the test apparatus:

- A 500 W fuel cell model Exergy FC_0.5.2, equipped with manually operable auxiliaries;
- Electronic load Zentro Elektik mod. Ela500;
- 4-channel digital oscilloscope Yokogawa DL1600;
- 3 current clamps;
- 48 V 40 Ah battery pack
- DC/DC converter.

3.2.2 Tests

The electronic load has been installed in order to simulate the engines of the UAV. The current clamps measured the current of the fuel cell, the batteries and the load. Voltage measurements were performed on the load side in order to evaluate variations of the latter caused by the engines. 3 particular cases have been investigated:

1. sudden load change;
2. sudden load interruption;
3. fuel cell system breakdown with shift to battery.

The behavior of the system in the case of sudden load changes is reported in fig. 2. It is worth noting that when the load (fig. 2a) is switched on, the current supplied by the fuel cell (fig. 2b) does not instantly follow the load requirements, but increases with a rate of 10 A/s. Because of the sudden load change, the voltage decreases (fig. 2c) and the battery (fig. 2d) provides the required power until the fuel cell is at full capacity, as evidenced by a negative current. When the load (fig. 2a) is switched off, the power demand from the stack is immediately reduced, as confirmed by the decreasing values of the current (fig. 2b). As a consequence, the load voltage increases (fig. 2c) and that the battery current becomes positive (fig. 2d) because all the power of the fuel cell is used to charge the battery.

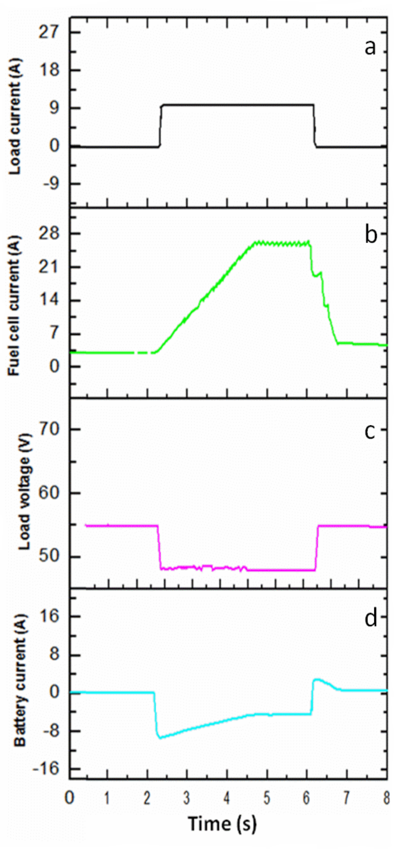

Fig. 2 Behavior of the system in the case of a sudden load increase. Variations of a) current requirements of the load, b) current supply by the fuel cell, c) load voltage and d) current provided to or absorbed by the battery.

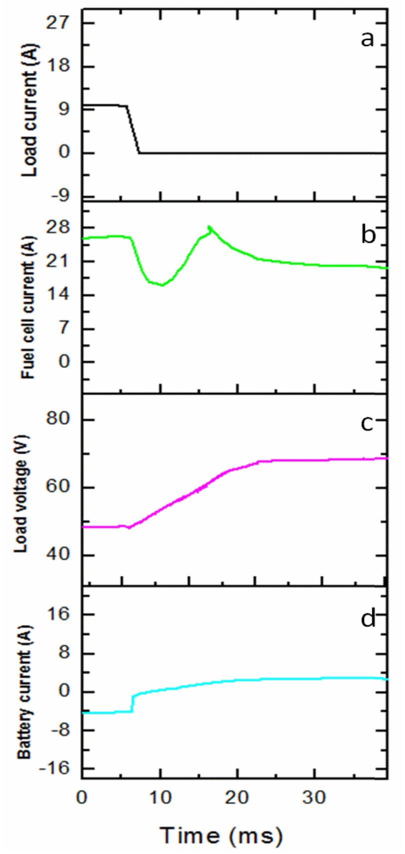

Fig. 3 Behavior of the system in the case of load interruption. Variations of a) current requirements of the load, b) current supply by the fuel cell, c) load voltage and d) current provided to or absorbed by the battery.

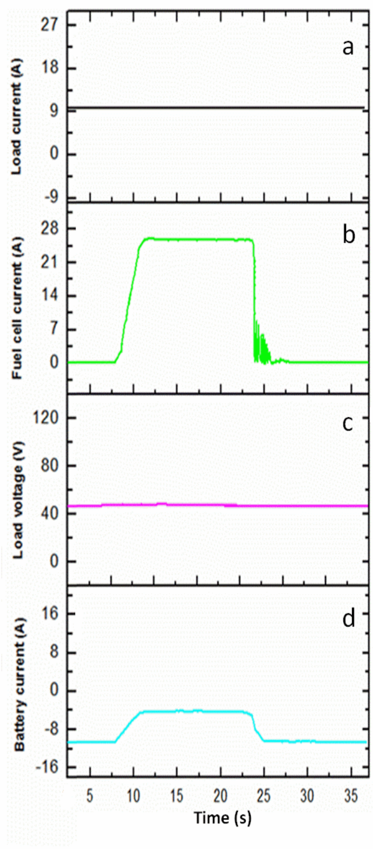

Fig. 4 Behavior of the system in the case of failure of the fuel cell. Variations of a) current requirements of the load, b) current supply by the fuel cell, c) load voltage and d) current provided to or absorbed by the battery.

In the case of a load interruption, reported in fig. 3, the response of the systems to the variation is significantly faster and for this reason the time scale in this case is in ms. When the power drops down (fig. 3a), the current taken from the fuel cell (fig. 3b) abruptly decreases and after a 10 ms oscillation, it increases again. At the same time an increase in potential of the engines bus (fig. 3c) is observed because the current of the battery (fig. 3d), that was supplying power, is put into charge. This transient lasts about 15 ms and, in this case, the fuel cell's current variation has been significantly faster than the preset rate (i.e. 10 A/s).

In the last case, reported in fig. 4, the behavior of the system in the case of fuel cell failure is investigated. Maintaining the current requirement from the load constant (fig. 4a), at the beginning, only the battery is providing power. After about 10 s, the fuel cell is activated (fig. 4b) and, because pf the constant value of the load voltage (fig. 4c), the battery current decrease in absolute value (fig. 4c), still remaining negative. The breakdown was simulated at about 25 s, by interrupting the hydrogen supply, so that the power output of the fuel cell resulted lower than the minimum value set by the controller. The oscillations visible for the fuel cell's current (fig. 4b) are due to the repeated attempts of the DC/DC converter to get power supply from this side. As more current is requested, the power of the fuel cell decreases until a critical value, causing an interruption of current. After 10 attempts the fuel cell is excluded. It is worth noting that, in order to maintain constant the load current (fig 4a) the battery recovered the initial value of the current (fig 4d), in order to keep the engines running.

4 System design

In the following paragraphs the sizing of the main components of the system will be described. In particular, according to the results of the flight and bench tests, the size of the fuel cell will be defined. Payload issues dictate the choice of a particular type of fuel cell as well. Another point in which payload plays a determining role is the hydrogen storage tank. In fact, the fuel must be enough to guarantee a sufficient flying range of the device, but, because lacking of a suitable infrastructures, the maximum pressure of the fuel into the tank is limited.

4.1 Drone

Although the flight tests (paragraph 3.1) were carried out with a hexacopter, it was decided to consider a coaxial octocopter. With respect to a hexacopter, in fact, an octocopter has a higher stability, which is a significant advantage for image acquisition in order to avoid obtaining blurred images. Another advantage of octocopters is the power of engines, that allow them to carry heavy loads. The main disadvantages are its dimensions and weight, which strongly affect the flying range and increases the cost, with respect to the other layouts. To solve this problem, a coaxial configuration is suggested. This configuration, which is obtained by mounting two rotors turned in opposite directions on every arm of the drone [23] is expected to provide an enhanced stability, an increased flying range and to allow transporting an increased payload.

The calculations for the sizing were performed by means of eCalc, a tool for calculations, simulations and design of electric motor driven systems for remote controlled models [24]. Focusing on the rotor and the airscrews, there's availability of a wide range of models, differing on size, power and payload: the selected rotor is U-10 model by T-MOTOR [25], with a 29" airscrew. It must be pointed out that the airscrew, and in particular its size, have a significant effect on the working of the motor. In particular, this airscrew-motor coupling has the following features (Tab. 2):

Engine	Tigermotor U-10
Airscrew	29”
Voltage	22.2 V
Current	4.1 A
Nominal power	91 W
Max payload	1.47 kg
rpm	1360

Tab. 2 Features of the motor-airscrew coupling, reference data at 65% of maximum power [25].

The choice has been made taking into account that the drone will carry about 12 kg load in total, trying to limit as much as possible electricity consumption. To allow a device of this weight to fly at a constant speed, in conditions similar to those described in fig. 1, a power of at least 750 W is needed. The total power requirement is 728 W; the auxiliary equipment, i.e. electro valves, cooling fan, etc., uses the remaining 22 W. These components are supposed to be powered by the auxiliary battery, even though battery and fuel cell work in parallel.
An aluminum-carbon fiber structure has been chosen, as these are the most commonly used materials for multirotor drones of comparable size [26].

4.2 Fuel Cell

A preliminary analysis was carried out on commercial fuel cells in order to evaluate the state of the art of these devices. The parameters taken into account were: operating temperature, membrane type, power output, fuel consumption, dimensions and weight. Considering that, for UAV application, weight is a critical issue, the number of components needed for the fuel cell to operate must be minimized. This has a first consequence on the cooling fluid: if it is air, only an additional blower will be needed instead of a complete cooling liquid circuit. Furthermore, if the membrane is of dry-type, and thus does not need to be humidified, it is possible to simplify the fuel line, further limiting the weight. An analysis of the characteristic of the fuel cell with wet-type membrane was performed for a Ballard fuel cell [27] and the results are shown in Tab 3, in which the weight without cooling fluids and cooling systems are reported versus power. It is evident that weights are high and are not suitable for the selected application.

Weight (kg)	Power (kW)
7.1	3.8
7.2	4.8
10.7	10.5
13	14.3
15	17.2
17	21.0

Tab 3: weight and power for Ballard fuel cells with wet-type membrane

According to these considerations, the commercial Horizon Aerostack [28] was selected for a possible development of the drone. The main features of the selected fuel cell are listed in Tab. 4.

Model	Aerostack Horizon
Nominal power	1 kW
Performance	30 V @ 33.5 A
Hydrogen consumption	14 l/min @ 1 bar
Dimensions	22 x 16 x 12 cm
Weight	2.0 kg

Tab. 4 Features of the PEM fuel cell [28].

The main advantage of this stack with respect to similar ones is its low weight: 2 kg including control units and blower, which acts as coolant and compressor for the air that enters into the fuel cell. It is noticeable that the fuel cell has 1 kW power output, while the engines of the drone have lower power consumption, as reported in paragraph 4.1. The excess power, in effect, will be used to charge the auxiliary battery.

4.3 Hydrogen storage

As previously reported in paragraph 4.2, the nominal power of the fuel cell is 1 kW and corresponding hydrogen consumption is 14 l/min at 1 bar at full load. Considering a flying range of 120 min, 1680 l of hydrogen at 1 bar are needed. However, an excess of fuel is usually stored into the tank, thus a total of 1800 l is considered to be contained in the tank. According to the operating pressure of the tank, different sizes can be defined, ranging from 8.0 l at 210 bar, up to 2.4 l at 700 bar. An operating pressure of 700 bar would be obviously the best solution in order to use the smallest, and thus lightest, tanks. On the other hand, a 700 bar operating pressure implies a multi step pressure reduction down to 1 bar for feeding the fuel cell and a dedicated infrastructure for the refilling of the tanks, which is not widespread. A 300 bar operating pressure was thus chosen, since it represents a good compromise between size of the tank (5.6 l) and an easy filling. Thus 2 tanks with a capacity of 3.0 l each have been planned. They are type III hydrogen tanks [29], with an aluminum liner, wrapped into an epoxy resin and carbon fiber composite, and have a weight of 1.2 kg each.

4.4 System powered by fuel cell and by batteries

In fig. 5a, a scheme of the system powered by fuel cell is reported, together with the list of its components.

The drawing reported in fig. 5a represents only the main structure of the hydrogen – fuel cell UAV system, without considering the structure of the drone, the camera and other components of the image acquisition system.

For comparison with the fuel cell powered system, a commercial Li-ion powered UAV has been considered, as this system represents the state of art of UAVs for this size and thus the direct competitor of the fuel cell-powered system on the market. The scheme of the system powered by batteries is reported in fig 5b. It differs from the previous one only for the power system, while the main components remain unvaried.

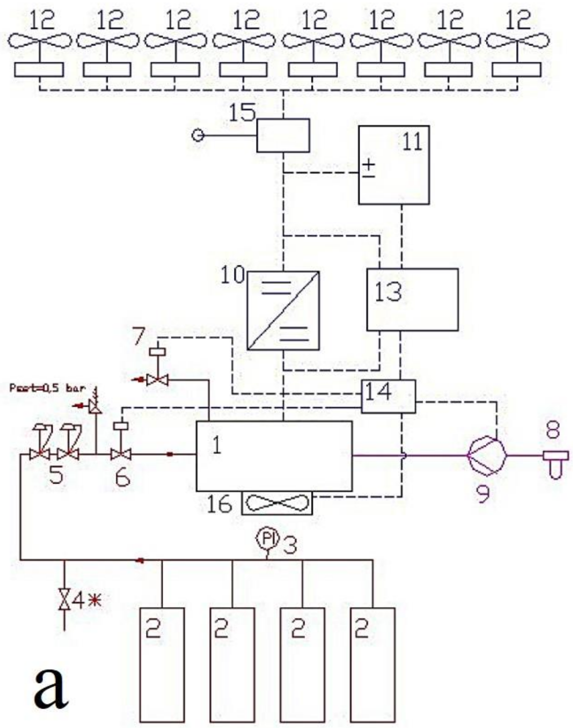

Item	Description
1	Fuel cell with controller
2	Hydrogen tanks
3	High pressure gauge
4	Refill valve
5	Pressure reducer
6/7	Electrovalves
8	Air filter
9	Air compressor
10	DC/DC converter
11	6800 mAh battery
12	Airscrews
12	Electric engines
13	Power management electronics
14/15	Power distribution boxes
16	Cooling fan

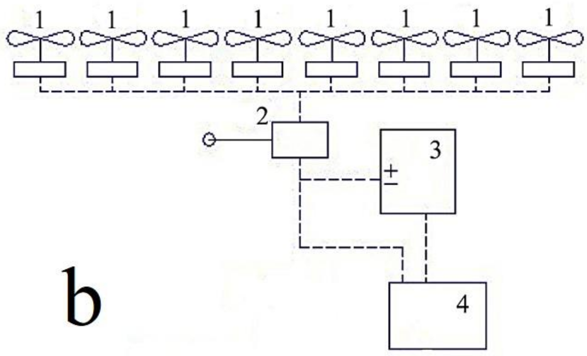

Item	Description
1	Airscrews
1	Electric engines
2	Power distribution boxes
3	Battery
4	Power management electronics

Fig. 5: a) scheme of UAV system powered by fuel cell; b) scheme of UAV system powered by batteries.

For the fuel cell and battery powered systems, a weight analysis was performed and the results are reported in Tab. 5 and Tab. 6, respectively. For the battery system, a specific energy of 0.250 kWh/kg has been considered.

Item	**Component**	**Quantity**	**Total weight (g)**	**Weight %**
12	Electric engines	8	3200	30.6
12	Airscrews	8	1120	10.7
1	FC controller	1	1900	18.2
9/16	Air compressor and cooling fan	1	170	1.6
2	Hydrogen tank	2	1740	16.7
	Tubing and connectors	1	150	1.4
5	Pressure reducer	1	170	1.6
3	High pressure gauge	1	30	0.3
	High pressure gauge	1	30	0.3
	HD Camera	1	700	6.7
	Motors support	1	300	2.9
6/7	Electrovalves	2	100	1.0
11	6800 mAh battery	1	163	1.6
	Chassis components	2	100	1.0
15	Power distribution boxes	2	100	1.0
	Security gauge	1	70	0.7
10	DC/DC converter	1	200	1.9
8	Air filter	1	50	0.5
13	Power management electronics	1	150	1.4
		Total	**10433**	

Tab 5 weight analysis for the FC powered system

Item	Component	Quantity	Total weight (g)	Weight %
1	Electric engines	8	3200	27.4
1	Airscrews	8	1120	9.6
	HD Camera	1	700	6.0
	Motors support	1	300	2.6
3	Li-ion battery 1.5 kWh	1	6000	51.4
	Chassis components	2	100	0.9
2	Power distribution boxes	2	100	0.9
4	Power management electronics	1	150	1.3
		Total	**11670**	

Tab 6: weight analysis for the battery powered system

The total weight of both systems is rather similar. It is evident that, in both cases, the main weight contribution is due to the used power system. Even if the fuel cell itself has a relatively limited weight, it requires the presence of hydrogen tanks and many other auxiliary components that increase the whole weight of the power system.

5 Cost analysis

In order to estimate the cost of the above-described systems, a cost analysis for the fuel cell-powered drone and the commercial Li-ion powered UAV has been performed.

The approximate costs of the components for both drones are listed in table 7, where X and – correspond to components used or not, respectively, for the two systems.

Component	Fuel cell drone	Battery drone	Cost (€)	Location
Complete fuel cell system	X	-	13300	Drone
Type III gas cylinders 2 x 3 l (@ 300 bar)	X	-	2240	Drone
Li-ion battery 1.5 kWh	-	X	1200	Drone
Engines and structure of the drone				
T motor U10 engines	X		2850	Drone
Motors supports			240	Drone
Airscrews			1600	Drone
Chassis components			1200	Drone
Auxiliary components				
Power distribution box	X		60	Drone
Regulators			320	Drone
Parachute			850	Drone
Cables			120	Drone
Power management electronics			350	Drone
DC/DC converter	X	-	150	Drone
Two-stage pressure reducer for hydrogen	X	-	850	Drone
Tubing, connectors, etc.	X	-	500	Drone
Li-ion battery 6800 mAh 3.7 V	X	-	50	Drone
Drone control and image acquisition				
GPS	X		110	Drone
Telemetry kit			220	Drone
HD camera			800	Drone
TX radio control			390	Ground
Flight terminator			450	Ground
Flight control computer			380	Ground
TX video			70	Ground
5.8 GHz Monitor			280	Ground
Monitor support			30	Ground
Total	**27410 €**	**11320 €**		

Tab. 7 Costs of the components of the fuel cell and battery powered drones .

It is immediately noticeable that the fuel cell-powered drone has the highest cost, that is more than double with respect to the battery-based one. This is mainly due to the cost of the fuel cell, which contributes for 49% to the total price of the system. In fact, while Li-ion batteries are already commercialized on large scale, fuel cells are still niche products. Furthermore, in the case of this study, a lightweight PEM fuel cell was considered, which is suitable for mobile applications. The same type of fuel cell, of the same manufacturer, but for stationary use is available at 1/3 of the former's price. This difference is due partly to the use of lightweight materials for mobile applications, and partly to the fact that, according to some features of the fuel cell which correspond to different application possibilities (i.e. stationary or mobile), there are different grades of diffusion on the market, and these have a huge influence on the current price of the product.

6 Environmental impact

Life Cycle Assessment (LCA) is an important tool to evaluate the environmental impact of a product, and follows the ISO 14040 /14044 methodology [30,31]. In the case of drones, as already mentioned, no former LCA studies on their production are available, even though the use of these devices, is more and more widespread thanks both to the availability of small models for hobbyists, and to the increasing interest for these devices by some goods distributing companies. The diffusion of UAV's for commercial purposes determines the necessity of a Life Cycle Assessment study in order to establish the corresponding energy and environmental implications [32].

6.1 Goal and scope

The goal of this LCA study is to give an indication of the environmental impacts of the components of the two types of UAVs from the raw material extraction through to the products end of life (cradle-to-grave) and their use, thus individuating possible bottlenecks. The analysis will involve the production of the two UAVs sized for a flying range of 120 minutes, without the control and image acquisition systems. In addition, the impact of their use, which implies electricity consumption for battery charging (for the battery-powered UAV) and hydrogen consumption and maintenance of the fuel cell (for the fuel cell-powered system), will be considered. The maintenance of the other parts of the drones, which consists mainly in the replacement of some components after a fixed number of operating hours, will not be considered due to the lack of data. It is however estimated that the impact of maintenance is small with respect to other phases. This statement seems to be confirmed by other LCA studies on PEM fuel cell or battery vehicles in which the impact of maintenance is not considered [33-35].

The analysis was performed by means of the commercial software SimaPro v 8.2 [36]. ILCD midpoint 2011 [37] as assessment method has been chosen.

6.2 Inventory

The data used for this study are taken from Ecoinvent database [38]. In the following paragraphs the performed assumptions are briefly described.

6.2.1 Fuel cell

As formerly discussed in 4.2, the fuel cell is a 1 kW PEM fuel cell, made for lightweight applications. Since the latter are still quite uncommon, a 2 kW PEM fuel cell made for stationary use has been considered. The main difference between the two devices lies in the air-cooling and self-humidification of the lightweight PEM fuel cell, which allows a weight reduction [28]. Since, according to previous studies [35, 39, 40] and due to the platinum group metals used, the most impacting components of fuel cells are the electrodes but not the auxiliary equipment for cooling and humidification, considering a stationary PEM fuel cell instead of a lightweight seems a reasonable choice.

6.2.2 Battery

The considered battery-powered UAV is equipped with a Li-ion battery. A $LiMnO_2$ battery from Ecoinvent database has been considered for this case. This battery, consisting in 14 cells, is able to produce 2 kWh energy output at 48 V. This is a typical electric car battery [38] but is considered suitable for UAVs as well [32].

6.2.3 Gas tanks

Data on the materials of the type III hydrogen tanks were taken from a previous LCA study by Gerboni et al. [41], where a bigger tank was considered. It is expected that the weight percentage of the materials of the tank do not vary with the size of the latter. The inventory for the tank is shown in tab. 8.

All the data are taken from Ecoinvent [38], but data for carbon fibers were taken from GaBi database [42].

Material	**Quantity (kg)***	**Data used**
Aluminum liner	1.45	Aluminum production Aluminum sheet rolling
Carbon fiber	1.21	Carbon fiber production
Epoxy resin	0.807	Liquid epoxy resin production

* The quantities refer to the total amount of materials of two tanks.

Tab. 8 Inventory for the gas tanks

6.2.4 Engines and structure of the drone

Copper coils into a carbon fiber structure, with carbon fiber airscrews, compose the engines of the drone. Carbon fiber is also a part of the structure, together with aluminum. The inventory for the engines and structure of the drone is shown in tab. 9.

Material	**Quantity (kg)**	**Data used**
Copper coils	1.6	Copper production Copper wires drawing
Carbon fiber	2.92	Carbon fiber production
Aluminum	0.3	Aluminum production Aluminum impact extraction

Tab. 9 Inventory for the engines and structure of the drone.

6.2.5 Auxiliary components

This category includes all the devices necessary for the operation of the drones, like hydrogen distribution circuit (including tubing, fittings, electrovalves, pressure gauge etc.), electronic components (printed circuit board, DC/DC converter), air filter, compressor and cooling fan.

Material/Component	**Quantity (kg)**	**Data used**
Printed circuit board	0.35	Printed wiring board for power supply unit
Stainless steel	0.33	Chromium steel production (secondary) Impact extrusion of steel
Plastics	0.30	Polyethylene production Injection-molding
Copper	0.17	Copper production
Titanium	0.17	Titanium production
Brass	0.07	Brass casting
Air filter	0.05	Polyethylene fleece

Tab. 10 Inventory for the auxiliary components.

For copper, titanium and brass, due to their low amount, only the metal/alloy production was considered without further processing. The auxiliary components are almost all referred to the fuel cell-powered drone, except for the printed circuit board, which is relative to both systems.

6.2.6 Use phase

In the use phase, hydrogen supply and electricity for battery charging are considered for the fuel cell-powered and the battery-powered UAVs, respectively.

The hydrogen used by the fuel cell is produced from hydrocarbon cracking in Europe, according to [38]. For battery charging, the Italian electricity mix has been chosen.

6.3 Results and discussion

Both production and use phase of a device may have significant impacts because of different reasons. If for the use phase fuel feedstock represents the main bottleneck, environmental impact of production is related to the use of particular materials, as well as energy intensive manufacturing processes. Due to these differences, in the following sections production will be first discussed separately from use.

6.3.1 Production.

From the results of impact assessment for Global Warming Potential (GWP) and Cumulative Energy Demand (CED), reported in fig. 6, it is possible to notice that one of the highest impacts for the fuel cell powered drone is given by the fuel cell itself. This is mainly due to the platinum extraction (60 % of the total impact), as confirmed also by other studies [39, 43-45] and to the treatment of the plastics of the fuel cell electronics at its end of life (14 % of the total impact). The LCA in fact considered also the energy required for this step on the final product.

The structure and engines of the drone give another significant impact. The origin of this impact is the carbon fiber (CF) used for both engines and structural parts, followed by copper used in the engines. The high impact of carbon fiber on both GWP and CED is mainly due to the energy intensive carbonization process of the polyacrylonitrile precursor [46,47]. Carbon fiber production has a significant contribution also on the type III gas tanks production even if less than that of aluminum production for the liner. The contribution of epoxy resin is negligible, due also to its small amount.

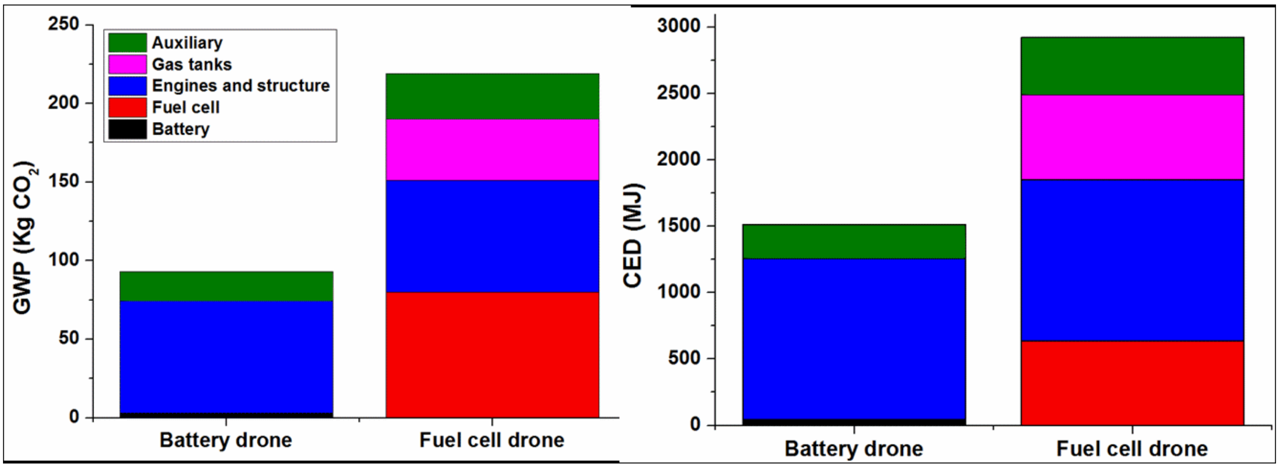

Fig. 6 Impact distribution of Global Warming Potential and Cumulative Energy Demand for the production stage of fuel cell and battery-powered drones.

The impact of the auxiliary components is mainly due to the assembly of the printed circuit, and in particular to the amount of copper used. Since this component is common to both UAVs, both show this contribution. In the case of the fuel cell-powered drone the metals used for valves, fittings, tubing and pressure gauge give another important contribution to the impact of the auxiliaries.

Noteworthy is the low impact of the Li-ion battery for the battery-powered drone. This contribution is due mainly to the energy intensive assembly process, together with the anode manufacturing, and in particular the use of graphite, as confirmed by other studies [44, 48]. Also in this case, as seen for the fuel cell, in addition to the impact of the production of the device, the impact of the battery disposal treatments was taken into account. The latter, in fact, contributes for about 35% on the global impact of the battery, in particular the pyrometallurgical treatment for the recovery of the non-ferrous metals contained in the battery.

6.3.2 Use

When the use phase of a device is studied, the expected lifetime has to be considered, in order to account the total amount of fuel or electricity used.

As lifetime for the fuel cell, 20000 h are considered, while for the battery 6700 h. Since the battery provides 1.5 kWh for 1.5 h flying range, the total amount of electrical energy used in 6700 h is 7035 kWh assuming 5% losses. The fuel cell-powered drone has a hydrogen consumption of 14 l/min, thus the total amount of hydrogen used in 20000 h is 16800000 l.

When analyzing the life cycle of a device it can be useful to express the impact assessment results divided by its expected lifetime hours. Being the impacts thus spread over the lifetime of the device they can become from high to acceptable, in the face of a long lifespan of the device. An example is shown in fig 7: the results for Global Warming Potential and Cumulative Energy Demand relative to the production and use phase are reported divided by the lifetime hours of the fuel cell and battery. It is immediately noticeable that the impact of production of the fuel cell-powered system is now similar to that of the battery-powered one (although these systems are not directly comparable): respectively 0.0109 kgCO_2/h and 0.0139 kgCO_2/h for GWP, and 0.146 MJ/h and 0.226 MJ/h for CED. The reason of this change is the different lifetime of the two devices, which is in fact longer for the fuel cell with respect to that of the battery.

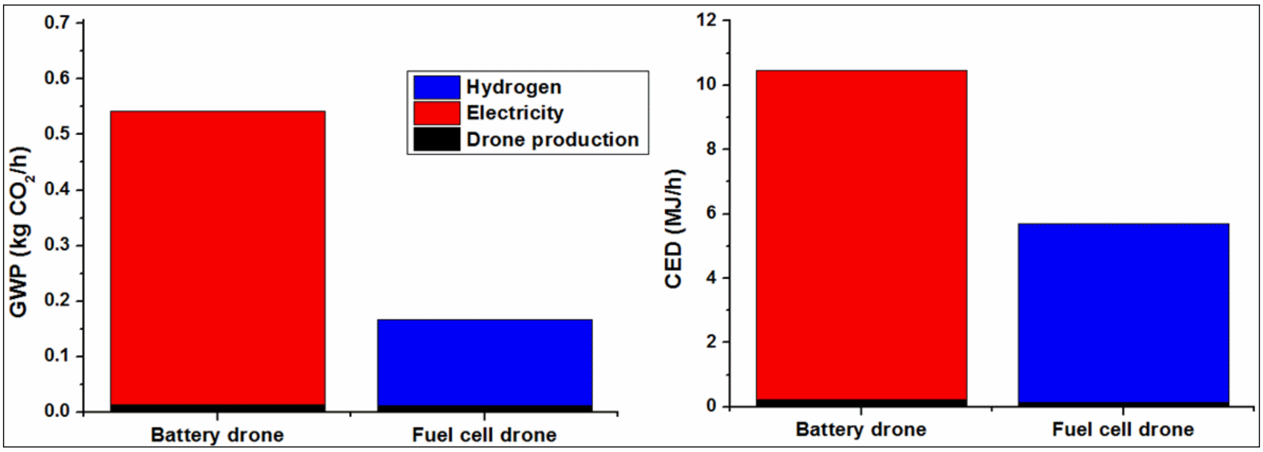

Fig. 7 Impact distribution of the considered life cycle stages for GWP and CED.

It is clear from fig. 7, that for both systems the use stage has a very high impact if compared with production. This kind of trend has also been observed in other LCA studies considering production and use of electric, fuel cell of internal combustion engines (ICE) powered vehicles [33-35].

The key role played by the electricity mix or hydrogen production method appears clear. In particular the Italian electricity mix is considered also in the study by Bartolozzi et al. [34], used for both battery charging and hydrogen production through electrolysis. In both cases, this electricity mix has higher impacts with respect to other sources considered in the study, such as gasification of biomass and eolic.

In a study by Bauer et al. [33], performing a comparison among different methods for electricity or hydrogen production from renewable and non-renewable sources, the authors concluded that both electric and hydrogen vehicles can reduce environmental burdens only if electricity and hydrogen are produced from renewable sources. The study by Donateo et al. [10] is particularly interesting as it estimates Well-To-Wing emissions associated to both battery-powered UAV and hydrogen-fueled PEM-powered one and concludes that CO_2 emissions are much greater when the powertrain is based on fuel cell particularly if hydrogen is obtained from electrolysis using the Italian electricity mix. The use of non renewable energy sources on the other hand could even increase the emission of greenhouse gases. Similar conclusions are drawn by Hwang [49].

7 Conclusions

In this study the use of a PEM fuel cell to extend the flying range of a coaxial octocopter is investigated. Also a battery-powered drone, which represents the state of art, is considered. For both systems, a cost analysis and life cycle assessment have been performed.

The cost of the battery-powered drone is certainly the most competitive, as this system is already commercially available and more simple, with respect to the fuel cell-powered. and the LCA results show that the battery has a very low environmental burdens if compared to other components of the same system, the main bottleneck in this case is the source of the electricity used for battery charging.

The main drawback of a battery-powered drone is the weight of the batteries, which increases with their size in order to extend the flying time becoming a limiting factor, as pointed out by Simic et al. [11]. In the case of a fuel cell powered drone, on the other hand, since the fuel cell size is fixed as it depends only on the features of the UAV, the limiting factor is given by the amount of hydrogen stored, which is determined by the volume of the pressure vessels and by their operating pressures. In this case, an operating pressure of 300 bar has been chosen due to the scarcity of refueling stations that allow to reach higher pressures. An operating pressure of 700 bar, already possible in refueling stations, could increase about twice the flying range. The main drawback of the fuel cell-powered system is however its high cost, which is more than twice that of the battery-based system, which is partly due to its increased complexity, but mostly to the still low commercial diffusion of fuel cells especially in the case of low weight stacks as the Aerostack considered for this study.

If use of drones is considered, it is worth noting that lifetime for fuel cells is about three times that of batteries. Therefore, a relative reduction of costs is observed if they are normalised by the lifetime hours of the systems. If 20000 h of drone use are considered, 3 batteries are needed and the total costs of the fuel cell and battery system are 27410 € and 13720 €, i.e 1.37 €/h and 0.69 €/h, respectively. Further costs reductions could be expected due to the continuous development and spread of fuel cell technology. Same observations can be carry out if environmental impacts are considered, so that, even if a direct comparison can not be easily performed, the impact of production of the fuel cell-powered system is similar to that of the battery-powered one if life time of the two systems is considered.

It can be concluded that the choice of a final user between the two considered systems will be mainly driven by a combination of flying time requirements and costs. If environmental impacts are considered, the balance between running time and cost of the drone becomes more challenge, suggesting a careful selection of applications and a life cycle impact analysis.

Acknowledgements
This work was performed in the framework of the Piedmont regional project "Dron-Hy", financed by FINPIEMONTE, POR-FESR Asse I, Attività I.1.3 Innovazione e P.M.I., Polo "Polight".

References

[1] Kim T., Kwon S., Design and development of a fuel cell-powered small unmanned aircraft. Int J Hydrog Energy 2012; 37: 615 – 622.

[2] Kim J., Kim T., Compact PEM fuel cell system combined with all-in-one hydrogen generator using chemical hydrides as a hydrogen source. Appl Energy 2015; 160: 945-953.

[3] Bhardwaj A., Samb, L., Akanksha, Martín-Torres, F.J., Kumar, R. Review: UAVs as remote sensing platform in glaciology: Present applications and future prospects. Remote Sens Environ 2016; 175: 196–204.

[4] Rokhmana, C.A. The potential of UAV-based remote sensing for supporting precision agriculture in Indonesia. Procedia Environ Sci 2015; 24: 245–253.

[5] Gago J., Douthe C., Coopman R.E., Gallego P.P., Ribas-Carbo M., Flexas, J., Escalona J., Medrano H., Review UAVs challenge to assess water stress for sustainable agriculture. Agric Water Manag 2015; 153: 9–19.

[6] Stöcker C., Eltner A., Karrasch P., Measuring gullies by synergetic application of UAV and close range photogrammetry—A case study from Andalusia, Spain. Catena 2015; 132: 1–11.

[7] Nishar A., Richards S., Breen D.; Robertson J., Breen B.. Thermal infrared imaging of geothermal environments and by an unmanned aerial vehicle (UAV): A case study of the Wairakei e Tauhara geothermal field, Taupo, New Zealand. Renew. Energy 2016; 86: 1256–1264.

[8] Doshi A. A., Postula A. J., Fletcher A., Singh S. P.N. Development of micro-UAV with integrated motion planning for open-cut mining surveillance. Microprocess Microsy 2015; 39: 829–835.

[9] Fernández-Lozano J., Gutiérrez-Alonso G. Improving archaeological prospection using localized UAVs assisted photogrammetry: An example from the Roman Gold District of the Eria River Valley (NW Spain), J of Archaeol Sci 2016;5: 509–520.

[10] Dudek M., Tomczyk P., Wygonik P., Korkosz M. , Bogusz P., Lis B., Hybrid Fuel Cell – Battery System as a Main Power Unit for Small Unmanned Aerial Vehicles (UAV). Int J Electrochem Sci 2013; 8: 8442 – 8463.

[11] Traub, L.W. Range and endurance estimates for battery-powered. J Aircraft 2011; 48: 703–707.

[12] Donateo T., Ficarella A., Spedicato L., Arista A., Ferraro M. A new approach to calculating endurance in electric flight and comparing fuel cells and batteries. Appl Energy 2017; 187: 807-819.

[13] Simic M., Bil C., Vojisavljevic V., Investigation in wireless power transmission for UAV charging. Procedia Comput Sci 2015; 60: 1846 – 1855.

[14] Rajendran P., Smith H. Implications of longitude and latitude on the size of solar-powered UAV. Energ Convers Manage 2015; 98: 107–114.
[15] Chang T., Yu H. Improving Electric Powered UAVs' Endurance by Incorporating Battery Dumping Concept. Procedia Engineer 2015; 99: 168 – 179.
[16] Renau J., Barroso J. , Lozano A., Nueno A., Sánchez F., Martín J., Barreras F. Design and manufacture of a high-temperature PEMFC and its cooling system to power a lightweight UAV for a high altitude mission Int j hydrog energy 2016;41: 19702 - 19712.
[17] Bradley T. H., Moffitt B. A., Mavris D. N., Parekh D. E. Development and experimental characterization of a fuel cell powered aircraft J Power Sources 2007; 171: 793–80.1
[18] Guida D., Minutillo M. Desigh methodology for a PEM fuel cell power system in a more electrical aircraft. Appl Energy 2017; 192; 446-456.
[19] Pregelj B., Micor M., Dolanc G. Petrovčič J., Jovan V. Impact of fuel cell and battery size to overall system performance - A diesel fuel cell APU case study. Appl Energy; 182: 365-375.
[20] Pregelj B., Micor M., Dolanc G. Petrovčič J., Jovan V. A model-based approach to battery selection for truck onboard fuel cell-based APU in an anti-idling application. Appl Energy 2015; 137: 64-76.
[21] Oliver Gröger,Hubert A. Gasteiger, and Jens-Peter Suchslandc, Journal of The Electrochemical Society, 162 (14) A2605-A2622 (2015)
[22] Williams, M.C., Suzuki, A., Miyamoto, A. Assessment of the performance of fuel cells and batteries, ECS Transactions; 2013; 51 (1): 183-192.
[23] Coleman C.P. A survey of theoretical and experimental coaxial rotor aerodynamic research. NASA technical paper 3675, 1997.
[24] ECALC, available at: http://www.ecalc.ch/index.htm, accessed on 5/10/2016.
[25] T-MOTOR, http://www.rctigermotor.com/, accessed on: 10/10/2016.
[26] http://www.flytop.it/prodotti, accessed on: 10/10/2016.
[27] Ballard product specifications available at http://www.ballard.com/docs/default-source/motive-modules-documents/material-handling/fcvelocity-9ssl.pdf?sfvrsn=2
[28] Horizon product specifications available at http://www.horizonfuelcell.com/, accessed on: 10/10/2016.
[29] Lagault M., Pressure vessel tank types, Composites World (2012), available at http://www.compositesworld.com/articles/pressure-vessel-tank-types.
[30] ISO 14040-environmental management – life cycle assessment – principles and framework. Geneva; 2006.
[31] ISO 14044-environmental management – life cycle assessment – requirements and guidelines. Geneva; 2006.

[32] Stolaroff J. K. The Need for a Life Cycle Assessment of Drone-Based Commercial Package Delivery. Lawrence Livermore National Laboratory, March 26, 2014, LLNL-TR-652316, available at: https://e reportsext. llnl.gov/pdf/772743.pdf, accessed on: 25/11/2016.
[33] Bauer C., Hofer J., Althaus H.-J., Del Duce A., Simons A. The environmental performance of current and future passenger vehicles: Life cycle assessment based on a novel scenario analysis framework. Appl Energy 2015; 157: 871–883.
[34] Bartolozzi I., Rizzi F., Frey M. Comparison between hydrogen and electric vehicles by life cycle assessment: a case study in Tuscany, Italy. Appl Energy 2013; 101: 103–11.
[35] Simons A., Bauer C. A life-cycle perspective on automotive fuel cells. Appl Energy 2015; 157: 884–896.
[36] SIMA PRO 8, LCA software, in http://www.pre.nl/simapro/simapro_lca_software.htm.
[37] General guide for life cycle assessment - detailed guidance. In *International reference life cycle data system (ilcd) handbook*, 1st ed.; European Commission - Joint Research Centre: Luxembourg. Publications Office of the European Union, 2010.
[38] Ecoinvent version 3.3 database, 8005 Zurich, Switzerland.
[39] Pehnt M. Life-cycle assessment of fuel cell stacks. Int J Hydrog Energy 2001; 26: 91 - 101.
[40] Sorensen B. Total life-cycle assessment of PEM fuel cell car, Paper 3e1189. In: Proc. 15thWorld Hydrogen Energy Conf., Yokohama. CDROM, World Hydrogen Energy Association; 2004.
[41] Gerboni R., Demaio N., Maffia L., Rossi S. LCA of a carbon fiber wrapped pressure vessel for auto motive applications. 6th International Conference on EcoBalance - EcoBalance2004 - 25-27 October 2004, Tsukuba, Japan.
[42] Thinkstep. GaBi database, information on carbon fiber available at: http://gabi-documentation-2017.gabi-software.com/xml-data/processes/d2e4cb14-c5fa-49a3-b6c2-840a2b860d63.xml, accessed on: 04/04/2017
[43] Garraín D., Lechón Y. Exploratory environmental impact assessment of the manufacturing and disposal stages of a new PEM fuel cell. Int J Hydrog Energy 2014; 39: 1769 – 1774.
[44] Belmonte N., Girgenti V., Florian P., Peano C., Luetto C., Rizzi P., Baricco M. A comparison of Energy storage from renewable sources through batteries and fuel cells: A case study in Turin, Italy. Int J Hydrog Energy 2016; 41: 21427-21438.
[45] Belmonte N., Luetto C., Staulo S., Rizzi P., Baricco M. Case Studies of Energy Storage with Fuel Cells and Batteries for Stationary and Mobile Applications. Challenges 2017; 8: 9.
[46] Harper International, Processing Advancements Within Reach for Achieving Significant Reductions in Carbon Fiber Cost of Manufacturing, JEC Europe 2013, ParisICS Carbon Conference, available at http://www.harperintl.com/wp-content/uploads/2011/09/JEC.pdf
[47] Song Y.S., Young, J.R., Gutowski T.G. Life cycle energy analysis of fiber reinforced composites. Compos Part App Sci Manuf 2009; 40: 1257-1265.

[48] Majeau-Bettez G., Hawkins T. R., Hammer Strømman A. Life Cycle Environmental Assessment of Lithium-Ion and Nickel Metal Hydride Batteries for Plug-In Hybrid and Battery Electric Vehicles. Environ Sci Technol 2011; 45: 4548–4554.

[49] Hwang J.-J. Sustainability study of hydrogen pathways for fuel cell vehicle applications. Renew Sust Energ Rev 2013; 19: 220-229.